Metallomics

RSC Publishing

PAPER

View Article Online
View Journal | View Issue

Cite this: *Metallomics*, 2013, **5**, 1276

Diverse accumulation and distribution of nutrient elements in developing wheat grain studied by laser ablation inductively coupled plasma mass spectrometry imaging†

Bei Wu,*[a] Franka Andersch,[b] Winfriede Weschke,[b] Hans Weber[b] and J. Sabine Becker[a]

Received 18th March 2013,
Accepted 3rd July 2013

DOI: 10.1039/c3mt00071k

www.rsc.org/metallomics

The present study focused on the elemental distribution in the developing wheat grain by using the laser ablation inductively coupled plasma mass spectrometry (LA-ICP-MS) imaging technique. Our studies show that the embryo accumulated high concentrations of nutrient elements, such as Fe, K, Cu, and Zn, while Ca was accumulated in the bran of the wheat grain which might be attributed to its function of structural maintenance. In the endosperm the majority of the nutrients were located in the aleurone layer. Within the grain, the embryo could be considered as a nutrient pool for macro- and micro-elements essential for the development of the seedling. Elemental images showed that considerable amounts of nutrients were stored in the scutellum of the embryo, which might be related to the high gene expression of element transporters in the scutellum. Root primordia and leaf primordia were enriched in particular elements, such as Mn and Zn respectively. In total 34 cross sections were analyzed and used for generation of a sequence of elemental distribution images to demonstrate elemental changes along the perpendicular axis of the wheat grain embryo. Further development of three-dimensional modeling will be combined with physiological studies to better understand the mechanisms of elemental distribution and storage in the wheat grain. These studies will provide fundamental knowledge on improving the nutritional value and agronomic practices.

1. Introduction

Micronutrients are indispensable for the normal plant development and are involved in all aspects of growth and metabolism such as energy metabolism, primary and secondary metabolism, cell protection, gene regulation, hormone perception, signal transduction and reproduction. The physiological importance of micronutrients was originally described on the basis of deficiency symptoms.[1] On the other hand, an excess of many micro-elements (*e.g.* Cu, B) is toxic. Plants have to maintain homeostasis of micronutrients, which requires a network of mobilization, uptake and distribution within the plant, intracellular trafficking, and storage. Metals in plants are often chelated by phytate or nicotianamine.[2] Storage of micronutrients in seeds is especially important to supply the growing seedling after germination. It is also important to understand the uptake and distribution of micronutrients in the wheat grain to improve the nutritional value, which can help to cope with the so-called hidden hunger. Malnutrition is a severe issue for a large amount of the world's population, especially for women and children. Nutrients obtained from the daily diet are limited in many places in the world. Crop grains and their flours are consumed as staple food and are one of the main sources of nutrient supply for human beings. Therefore, improving the quality of crops, preserving nutrients during food processing, as well as amending bioavailability of nutrients in crops, especially that of trace elements such as Cu, Zn and Fe, are important strategies to overcome nutrition deficiency. This requires a great deal of effort on both fundamental research and agronomic practices.

The distribution of micronutrients is highly regulated on the spatial and temporal levels. The distribution pattern of different

[a] *Zentralinstitut für Engineering, Elektronik und Analytik, Analytik (ZEA-3), Forschungszentrum Jülich (FZJ), D-52425 Jülich, Germany. E-mail: b.wu@fz-juelich.de; Fax: +49 2461 612560; Tel: +49 2461 615163*

[b] *Leibniz-Institut für Pflanzengenetik und Kulturpflanzenforschung (IPK), D-06466 Gatersleben, Germany*

† Electronic supplementary information (ESI) available: The successive visualization of the distributions of C, Cl, B, P, S, K, Ca, Na, Mg, Fe, Cu, Zn, Mn, and Mo is given separately as .avi files. The elemental concentrations in different grain organs are given in Table S1. See DOI: 10.1039/c3mt00071k

elements in seeds is variable indicating that transport and storage are specific for each element. Micronutrients are mainly translocated into seeds during the earlier developmental phases at 10 to 14 days after pollination.[3] Concentrations of Zn and Cu in the barley embryo are found to be four- to five-fold higher than those in the whole grain. The analysis of the spatial distribution of Zn and Fe by synchrotron-based X-ray fluorescence microscopy has identified the scutellum as the main accumulation organ in wheat and wheat embryos.[4]

Recently, mass spectrometric imaging techniques have created a new aspect of metallomic studies with respect to micro-local distribution of elements or molecules of interest in biological tissues. The distribution profiles of metals and non-metals and their species are combined to assist in understanding metabolic processes and bio-functions of an element or a molecule. For elemental imaging, laser ablation inductively coupled plasma mass spectrometry (LA-ICP-MS) has been successfully applied to investigate the distribution of metals/metalloids and non-metals such as P and C in various biological tissues such as rodent brain[5–7] and kidney[8,9] with or without diseases,[10] as well as plant tissues.[11,12] Because of its multi-elemental analysis properties, LA-ICP-MS imaging (LA-ICP-MSI) is capable of revealing most of the bio-relevant elements quasi-simultaneously. Other advantages of LA-ICP-MSI include simple instrumentation, operation in an ambient atmosphere, and easy sample preparation. In addition, only little matrix effect occurs in LA-ICP-MS, therefore, easy quantification procedures are possible *via* matrix-matched laboratory standards. The sensitivity of LA-ICP-MS imaging is sufficiently high that elements with concentration at the level of ppm ($\mu g\ g^{-1}$) and lower are detectable which allows the investigation of metabolic products at trace level.

In the present study, distribution of macro- and micro-nutrients in cross sections of wheat grain was analyzed by the LA-ICP-MS imaging technique to aid effective nutrition modification in crops.

2. Experimental

2.1 Sample preparation

Wheat plants were cultivated in green houses and developing caryopses were harvested as described in Weichert *et al.* (2010).[13] Wheat caryopses at 25 days after flowering (DAF) were frozen in liquid nitrogen and transferred to a cryotome (Bright Instrument Co Ltd, Huntingdon, England). Using a razor blade the embryo-containing part of caryopses was cut out and glued onto the sample plate by means of Tissue-Tek® O.C.T.™ compound embedding medium (Sakura Finetek Europe B.V., Zoeterwoude, The Netherlands). The embryo-containing part was cut into 26 μm thick serial sections. Cryosections were mounted on Superfrost microscope slides (Carl Roth KG, Karlsruhe, Germany) and stored until dryness for 7 days in the cryostat chamber at −20 °C.

The dried sections were photographed under a VHX-100K digital microscope (Keyence Corporation, Higashi-nakajima, Higashi-Yodogawa, Osaka, Japan). These microscopic photographs of the sections were used for histological recognition of the embryo structure and for visual registration of the ion images.

In order to illustrate the histology of the wheat grain embryo (Fig. 1), wheat caryopses (25 days after fertilization) were fixed in 4% para-formaldehyde, 10 mM DTT, PBS buffer, dehydrated, infiltrated and embedded in butyl-methyl methacrylate (BMM).[14] Three micrometer thick sections were generated using a rotary microtome and cross sections were mounted on Superfrost microscope slides (Carl Roth KG, Karlsruhe, Germany), and then stained with acridine orange. BMM was removed (2×10 min in acetone) and sections hydrated in an ethanol series (100, 70, 50, 30%, 2 min each), followed by washing in 1% acetic anhydride for 30 s, 0.1 M Sorensen's phosphate buffer at pH 6.0 for 2 min, 0.01% acridine orange in 0.1 M Sorensen's phosphate buffer at pH 6.0 for 3 min, 11% $CaCl_2$ for 30 s and then twice in Sorensen's phosphate buffer at pH 6.0 for 2 min. Sections were photographed using the fluorescence microscope (Zeiss Axio Imager M2 microscope, Carl Zeiss, Jena, Germany). Fig. 1a represents a schematic view of a wheat grain. Fig. 1b and c represent two sections of the embryo region (red color) at the layer of root primordia (Fig. 1b) and at the layer of the leaf primordia (Fig. 1c).

2.2 LA-ICP-MS imaging

LA-ICP-MS imaging of nutrient elements in the cross sections of the wheat grain was performed using a commercial laser ablation system (LA, New Wave NWR213, Fremond, CA, USA) coupled to a quadrupole-based ICP-MS (ICP-QMS, XSeries2, Thermo Fisher Scientific, Bremen, Germany). The LA system was equipped with a solid state Nd:YAG laser at wavelength 213 nm. The laser beam with a spot size of 25 μm and a fluence of 0.26 J cm^{-2} was used to scan the cross sections at a speed of 40 μm s^{-1}. The ablated materials were transported by Ar as a carrier gas to the inductively coupled plasma (ICP) where atomization and ionization of the transported sample material occurs. The positively charged ions of the extracted and accelerated ion beam were separated by their mass-to-charge ratio (m/z) in the mass analyzer. Spatially resolved elemental images were then generated along the laser scans.

For quantification purposes, the powder of ground wheat grains at 25 DAF was used. Portions of the powder were spiked with mixtures of standard solutions with known concentrations of the elements of interest. After absorption of the analytes for 48 h, the homogenates were dried at 75 °C in an oven, and then ground again into fine powder and pressed under 8 atm. The added element concentrations were diverse according to each element, from 0.05–0.5 $\mu g\ g^{-1}$ for micro-nutrients such as Mo, to 725–6250 $\mu g\ g^{-1}$ for macro-nutrients such as K. The prepared standards were validated as described previously.[11] The in-house standards were analyzed by LA-ICP-MS using line scans before and after measurement of each section under the same experimental conditions. The linearity of the calibration curves generated from these standards was found to be better than 0.99, with the lowest for Mo at 0.997 and the highest for Cu and Zn at 0.9999.

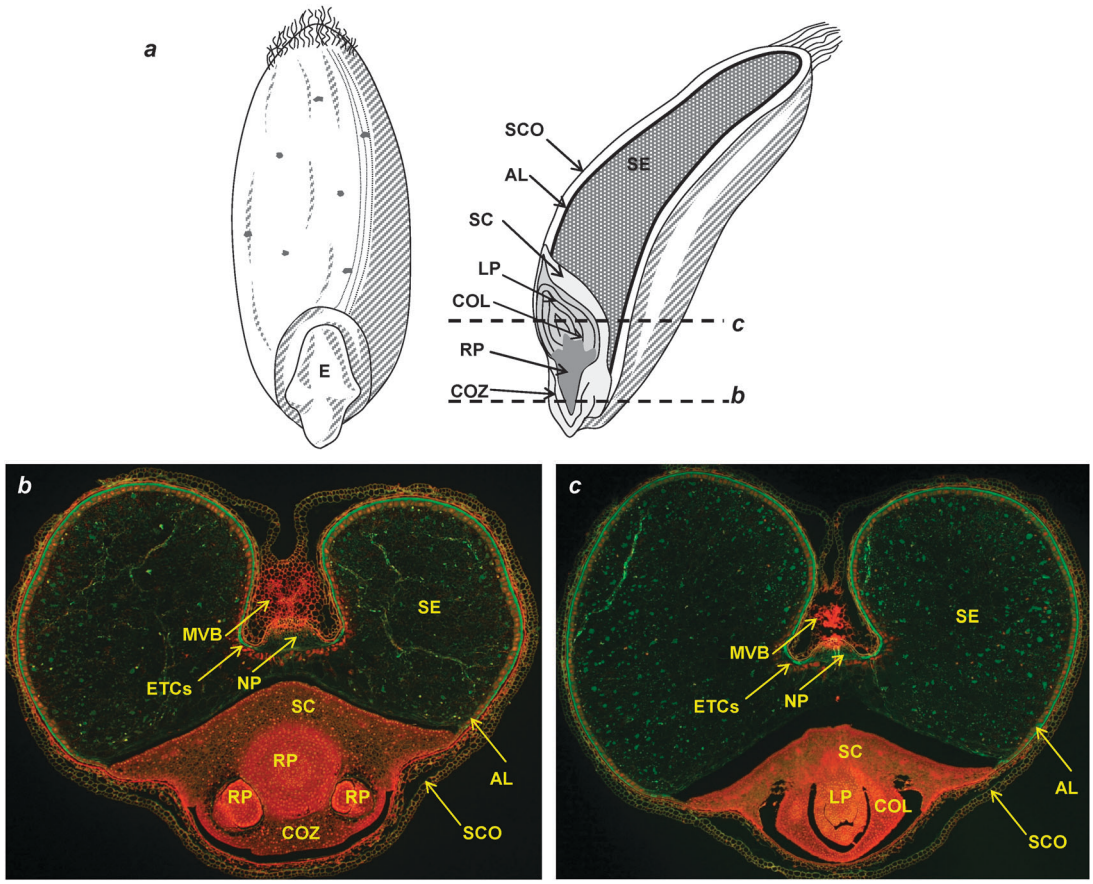

Fig. 1 Schematic view of a wheat grain (a) (left, front view; right, longitudinal section) and cross sections through a wheat grain at 25 DAF. Sections represent the embryo (red color) at the layer of root primordia (b) and at the layer of the leaf primordia (c). AL, aleurone; COL, coleoptile; COZ, coleorhizae; ETCs, endospermal transfer cells; LP, leaf primordia; MVB, main vascular bundle; NP, nucellar projection; RP, root primordia; SC, scutellum; SCO, seed coat; SE, starchy endosperm.

The ICP-MS was daily tuned using 10 ng g^{-1} standard solution containing multi-elements with respect to high ion intensity and stable signals of $^{7}Li^{+}$, $^{115}In^{+}$, and $^{238}U^{+}$. Simultaneously, oxide formation was controlled by limiting $^{232}Th^{16}O^{+}/^{232}Th^{+}$ to $<0.3\%$. The optimized LA-ICP-MS conditions are summarized in Table 1.

Table 1 Optimized experimental parameters used for LA-ICP-MS imaging of the cross sections of the wheat grain

ICP-MS	ICP-QMS, XSeries2, Thermo Fisher Scientific
RF power (W)	1500
Carrier gas flow rate (L min^{-1})	1.0
Mass resolution ($m/\Delta m$)	300
Isotopes measured	$^{10}B^{+}$, $^{11}B^{+}$, $^{13}C^{+}$, $^{23}Na^{+}$, $^{24}Mg^{+}$, $^{25}Mg^{+}$, $^{31}P^{+}$, $^{34}S^{+}$, $^{35}Cl^{+}$, $^{39}K^{+}$, $^{42}Ca^{+}$, $^{44}Ca^{+}$, $^{55}Mn^{+}$, $^{56}Fe^{+}$, $^{57}Fe^{+}$, $^{63}Cu^{+}$, $^{65}Cu^{+}$, $^{64}Zn^{+}$, $^{66}Zn^{+}$, $^{95}Mo^{+}$, $^{98}Mo^{+}$
LA system	New Wave NWR213, New Wave Research
Laser	Nd:YAG
Wavelength (nm)	213
Pulse width (ns)	20
Repetition rate (Hz)	20
Laser spot size (μm)	25
Scan speed (μm s^{-1})	40
Laser fluence (J cm^{-2})	0.26

2.3 Data processing

The ion intensity of measured isotopes were exported and converted into images with temporal and spatial information of the scanned areas using in-house software IMAGENA.[15] Each ion image was aligned with the corresponding microscopic photo with respect to image orientation and histological structure using the Fusion Tool in PMOD software (PMOD, v 3.13, Zurich, Switzerland). The PMOD software allowed averaging "values of interest (VOI)" in a defined region, so that the element concentration in sub-structures of the wheat embryo was calculated accordingly.

To study the variation of nutrients' distribution in the wheat embryo along the perpendicular axis, a total of 34 cross sections of the embryo region of the wheat grain were measured and quantified. Each ion image from IMAGENA was resized to 400 × 300 pi while the pixel size was kept constant, *i.e.* 1 pi, so that the generated pictures contained ion images with the actual dimensions of the relevant section. The visual registration of subsequent wheat sections was realized using PMOD software to generate a sequence of images for each element. The reconstructed image sequence was imported to Fiji Is Just

ImageJ (http://fiji.sc/) for consecutive visualization of the distribution pattern of each element from the location of the root primordia to that of leaf primordia in the embryo. The visualization was converted into an .avi file for each element, which is given as the ESI.†

3. Results

3.1 LA-ICP-MS imaging of cross sections of the wheat grain

A wheat grain of 25 DAF was cryo-cut into 26-μm thick sections perpendicular to the crease successively, so that the histology of each cross-section was preserved symmetrically while minor changes of the structure were present in adjacent sections. This stage at 25 DAF was chosen as it represents the late storage phase where starch and dry weight accumulation has reached its maximum.[16] At 25 DAF, pericarp cells are already disintegrated and the cells of the starchy endosperm undergo programmed cell death. The organs, which are still alive, include the embryo, the aleurone, the nucellar projection and the main vascular bundle.

The benefit of multielemental analysis of LA-ICP-MS was to simultaneously generate ion images of both macro- and micro-elements in the wheat grain section with concentrations ranging from sub μg g^{-1} (Mo) to >2% (P) of dry mass weight (Table 2). Direct sampling on a tissue section by the laser beam in the scanning mode produced continuous flow of the analytes temporal along the ablation, which could be aligned with the laser ablation position to create spatial distribution of the analytes of interest within the biological scale. Although the dimensions of the cross sections varied from 2.3 × 1.8 to 4.1 × 3.2 mm^2 in the studied slices (Fig. 1A), the LA-ICP-MS parameters such as the spot size of the laser beam, scan speed, acquisition time per data, *etc.* were kept constant for a spatial resolution of 25 μm for all the sections measured. The spatial resolution was sufficient to differentiate sub-regions of interest in the embryo. Moreover, the layers in the bran such as the seed coat were distinguished very well from the aleurone layer of the endosperm. The ion images of the analytes were quantified using matrix-matched laboratory standards prepared by the powder of wheat grains at 25 DAF.

Table 2 Average concentration of each nutrient element in the three main parts (the seed coat (SCO), the endosperm, and the embryo) of the wheat grain at the layers (n = 6) of root primordia (a) and at the layers (n = 6) of the leaf primordia (b) (see Fig. 1, Cl was not quantified)

	Concentration (μg g^{-1})		
Element	Seed coat	Endosperm	Embryo
(a)			
K	2916 ± 398	1661 ± 241	11 793 ± 1012
Ca	1114 ± 150	312 ± 37	628 ± 79
Mg	69 ± 5	505 ± 56	3293 ± 286
Na	41 ± 5	4.0 ± 0.7	28 ± 1
Mn	31 ± 5	5.6 ± 0.9	137 ± 12
Fe	7.3 ± 0.6	13 ± 1	79 ± 6
Cu	0.62 ± 0.09	2.3 ± 0.3	13 ± 1
Zn	15 ± 2	15 ± 1	158 ± 13
Mo	0.17 ± 0.02	0.17 ± 0.01	0.38 ± 0.04
P	1596 ± 184	2805 ± 154	23 423 ± 1047
S	704 ± 119	1508 ± 173	2858 ± 316
B	5.6 ± 1.0	0.47 ± 0.03	4.6 ± 0.2
(b)			
K	2791 ± 294	1620 ± 219	12 432 ± 1112
Ca	1101 ± 102	284 ± 31	568 ± 51
Mg	88 ± 7	441 ± 42	2955 ± 196
Na	46 ± 6	4.2 ± 0.6	25 ± 2
Mn	28 ± 3	4.8 ± 0.3	113 ± 9
Fe	6.1 ± 0.5	10 ± 1	75 ± 5
Cu	0.69 ± 0.08	2.6 ± 0.2	15 ± 1
Zn	13 ± 2	16 ± 1	184 ± 15
Mo	0.14 ± 0.01	0.14 ± 0.01	0.78 ± 0.01
P	1818 ± 217	3004 ± 294	22 238 ± 1321
S	609 ± 73	1310 ± 201	2481 ± 226
B	4.7 ± 0.8	0.36 ± 0.03	3.2 ± 0.2

The distribution of essential elements such as K, Ca, Na, Mg, Fe, Cu, Zn, Mn, Mo, P, S, B and Cl in two sections of the wheat grain is shown in Fig. 2 and 3, corresponding to the histological indication in Fig. 1, respectively.

All the elements measured, except for Ca, were considerably enriched in the embryo of the wheat grain, especially Mg and P averaged at 3600 ± 390 and 21 000 ± 3700 μg g^{-1} (n = 34) compared to those in the endosperm (including the aleurone layer) at 550 ± 90 and 2600 ± 360 μg g^{-1} (n = 34), respectively. Within the embryo the scutellum represented a particular structure which accommodated most of the nutrients such as Fe and Cu to support wheat seedling development. The average concentrations of Fe and Cu in the scutellum were 110 ± 19 and 18 ± 3 μg g^{-1} (n = 34), respectively. The Ca concentration was also high in the scutellum compared to other embryo tissues. High concentrations of nutrients in the embryo of the wheat grain have been found previously.[17] However, considering that the embryo makes up around 10% of the grain weight, the total nutrient content may be relatively low in the embryo compared to that in the endosperm.[17] The embryo is usually removed in the milling process because it contains lipids that limit the keeping qualities of flour.[18] This would result in loss of nutrients accessible from the crops.

In contrast, the cells of the starchy endosperm, which are filled with starch granules and proteins and which form the main source of the flour product, had the lowest concentration of the nutrients, except for S, which was abundant in the endosperm as well (Table 2 and ESI,† Table S1). Compared to the starchy endosperm, the aleurone cells, which form the outer layer of the endosperm, coated by the bran, accumulated relatively higher amounts of *e.g.* K and Ca. In the bran of the grain, elemental distribution in the sublayers varied according to the elements. K, Fe, Mg, Cu and P were located in the aleurone cells, while Na was enriched rather in the seed coat. Ca, Zn, Mo, and Mn in these two layers did not present significant differences. A high amount of Mo was observed in the region of the main vascular bundle and the nucellar projection.

3.2 Nutrient distribution in the wheat embryo

Potassium. Potassium is an essential nutrient for proper plant growth and reproduction and is present as a free cation (K^+) in the protoplasm and as a cofactor of enzymes. K is involved in cell expansion, osmo-regulation, the function of stomata,

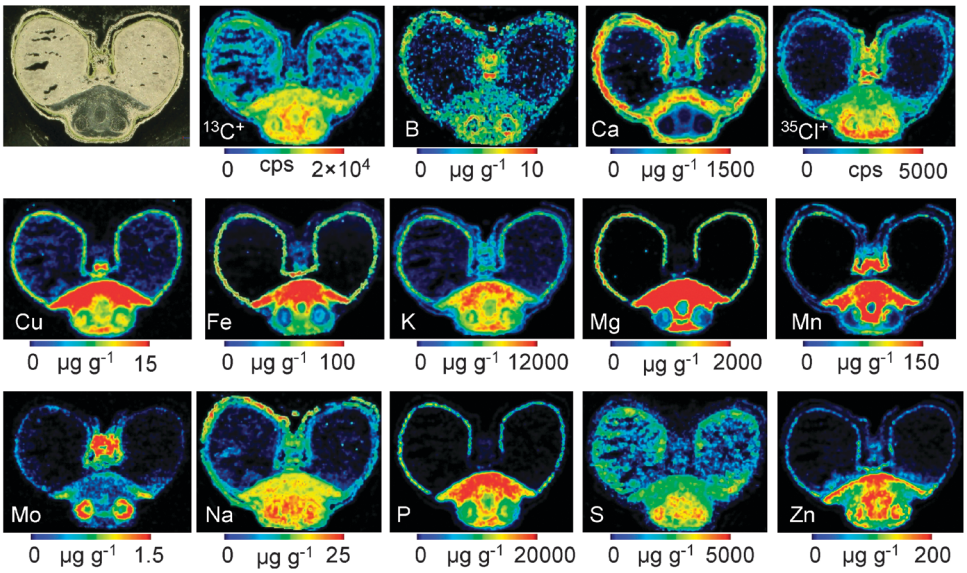

Fig. 2 Elemental distribution in cross sections of the wheat grain at the level of root primordia (see Fig. 1b).

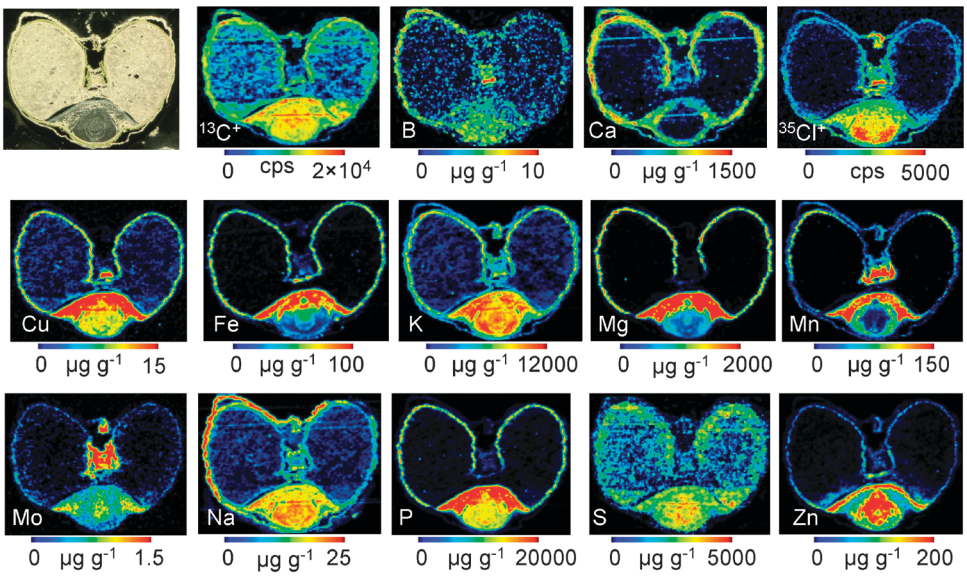

Fig. 3 Elemental distribution in cross sections of the wheat grain at the level of leaf primordia (see Fig. 1c).

and protein and starch synthesis where K activates respective enzymes. K also acts as a counter-ion during H^+-coupled co-transport of sucrose and amino acids.[19] In the wheat grain, K was enriched in the embryo, especially in the inner region of the scutellum and the coleorhizae and coleoptile, which was more than 16-fold higher than in the starchy endosperm (Table 2 and ESI,† Table S1).

Calcium. Unlike most of the metal ions, Ca in plants occurs as a free cation (Ca^{2+}). Within the plant, Ca is essentially required for the structural maintenance of cell walls and membranes. Ca acts as a counter cation in vacuoles and within the cytosol and serves as an intracellular messenger to coordinate development.[20] Within the wheat grains, Ca was considerably enriched in the seed coat and the aleurone, which could be attributed to the role of Ca in structural maintenance. Most of the Ca in the embryo was found in the scutellum, while only ~250 µg g^{-1} Ca was found in the root or leaf primordia.

Magnesium. In plants, Mg^{2+} is the metal ion in chlorophyll and in many enzymes, especially in energy metabolism such as ATP biosynthesis. Mg is also required in membranes and for pectin biosynthesis. Mg modulates ionic currents across chloroplasts and vacuolar membranes, and thus might regulate ion balances in the cell and stomatal opening. The vacuoles play a key role in Mg homeostasis.[21] In the wheat grain, as much as 4000 µg g^{-1} Mg was concentrated in the aleurone and the scutellum. In the root coleorhizae, the level of Mg was two fold higher than that in the root primordia. Similarly, Mg was less concentrated in the root primordia than in the leaf coleoptile.

Sodium. In plants, Na is present as a cation (Na^+) and involved in maintaining turgor homeostasis. At higher levels, Na is toxic, inhibits many enzymes and can also achieve osmotic and salt stress. Excess Na can detrimentally interact with K uptake and metabolism.[22] Na can be replaced by K in plants. However, the distribution pattern of Na in the wheat grain was found to be different from that of K. The seed coat was enriched in Na, the concentrations of which were comparable to that in the embryo. In the embryo, Na was slightly concentrated ($\sim$10% more) in the root and leaf primordia compared to the scutellum.

Manganese. Manganese is involved in the catalytic centre of more than 25 enzymes and can also activate enzymes such as super oxide dismutase.[23] Mn is required for photosynthesis and chloroplast biogenesis, organic acid, amino acid and nitrogen metabolism.[24] Mn also participates in gibberellic acid biosynthesis. It can be partially replaced by Mg. Similar to Mg, Mn was dominant in the scutellum of the embryo and low in the starchy endosperm of the wheat grain. However, in the coleorhizae, where Mg concentration was as much as twice that in the root primordia, Mn content was half of that in the root primordia. Both Mg and Mn were more highly enriched in the root primordia than in the leaf primordia. A particular location for Mn in the wheat grain was found in the endosperm transfer cells and the nucellar projection, where Mn concentration was as high as 450–520 $\mu g\ g^{-1}$.

Iron. In plants, Fe functions as a redox-active metal and as a component of Fe–S and heme-proteins. Fe-containing enzymes are involved in photosynthesis, mitochondrial respiration, nitrogen assimilation, hormone biosynthesis (ethylene, gibberellic acid, jasmonic acid), production and scavenging of reactive oxygen species, osmoprotection, and pathogen defense.[1] Around 80% of the plant Fe is found in the chloroplasts.[24] In the wheat grain, Fe was predominantly concentrated in the scutellum of the embryo and the aleurone layer of the endosperm. Compared with the leaf primordia, the root primordia accumulated relatively more Fe.

Copper. In plants, Cu is essential for photosynthesis, mitochondrial respiration, carbon and nitrogen metabolism, oxidative stress protection and cell wall synthesis.[1,24] Cu functions as a catalyst in many enzymes, especially in oxidases such as cytochrome C oxidase. Its metabolism is linked to that of Fe. The distribution pattern of Cu in the wheat grain resembled that of Fe. However, in root and leaf primordia Cu concentrations were at the same level of $\sim$10 $\mu g\ g^{-1}$.

Zinc. Zinc is important for enzymes of protein synthesis and energy production, and maintains the structural integrity of biomembranes. More than 1200 proteins contain, bind, or transport Zn such as Zn-finger containing proteins and transcription factors, oxidoreductases, and hydrolytic enzymes such as metallo-proteases. Many Zn-enzymes contain Zn-finger motifs and are involved in DNA-transcription, RNA-processing, and translation.[1,25] In the wheat grain, Zn was present in the aleurone, endosperm transfer cells, nucellar projection and main vascular bundle. The starchy endosperm contained a higher level of Zn in the region near the embryo but not in the remaining endosperm. Within the embryo, Zn was highly accumulated within a stripe at the dorsal region of the scutellum adjacent to the endosperm with the average concentration of $280 \pm 30\ \mu g\ g^{-1}$. Unlike Fe, Zn was enriched in the leaf primordia rather than the root primordia.

Molybdenum. As the only second-row transition metal with biological activity,[26] Mo is involved in nitrogen assimilation (nitrate reductase), sulphur metabolism, phytohormone biosynthesis, and stress reactions in plants. The last step of abscisic acid biosynthesis is catalyzed by the Mo-containing enzyme aldehyde oxidase.[1,27] Deficiency of Mo in plants might result in poor development of seeds.[26] Mo metabolism is linked to that of Fe and Cu. Different from other nutrient elements, Mo in the wheat grain was accumulated in the main vascular bundle and the nucellar projection, as well as in the lateral roots of the embryo. In the starchy endosperm Mo was present in the outer regions.

Phosphorus. As one of the most important nutrients for plants, P is a main constituent of nucleic acids and phospholipids, and involved in photosynthesis, energy metabolism and metabolic regulation by phosphorylation–dephosphorylation. Because P occurs in inorganic form and as a constituent of organic molecules, P locates at the branch point between organic and inorganic metabolism.[28] In the wheat grain P was the most abundant element with highest concentration in the scutellum above 3% of the dry weight. P was evenly distributed in the rest of the embryo with relatively high concentration in the coleorhizae.

Sulfur. In plants, S is one of the most important nutrients, and is a constituent of methionine and cysteine, and therefore present in most proteins. Plants synthesize special S-containing metabolites, such as glucosinolates, allylsulfur compounds, glutathiones and phytochelatins for biotic and abiotic stress defenses. Based on the importance of the wide range of S-containing metabolites and proteins the assimilatory pathways for S are tightly regulated in plants.[29] Although abundant S was present in the embryo of the wheat grain, it was the only element also enriched in the starchy endosperm with a downhill gradient towards the inner regions, which might reflect the accumulation pattern of S-rich storage proteins.

Boron. More than 90% of B in plants is found in cell walls, where it is involved in pectin synthesis, lignifications and as a component of wall polysaccharides such as rhamnogalacturonan.[30] B also participates in cell division, protein synthesis and in the regulation of carbohydrate metabolism and the structural integrity of cell walls.[31] B was present all over the wheat grain with the highest concentrations in the region of the nucellar projection and the main vascular bundle. Within the embryo, B was enriched in the coleoptile, leaf primordia and the outer layers of the lateral root primordia, potentially the rhizodermis/cortex region, and within the coleorhizae.

Chloride. Chloride (present in plants as Cl^-) is an essential nutrient and one of the most abundant inorganic anions in plant tissues. Cl is widely used as the major osmotic active solute in vacuoles. Cl participates in osmoregulation, cell elongation, enzyme activity regulation, stabilisation of membrane potential,

electrical charge balance and intracellular pH regulation.[30,32] From the ion image of $^{35}Cl^{+}$, it was shown that Cl was highly concentrated in the nucellar projection and the main vascular bundle of the wheat grain. Within the embryo, Cl was especially concentrated within the coleoptile and coleorhiza.

3.3 Successive visualization of elemental distribution patterns

In the present study, a total of 34 cross sections of the wheat grain with an interval space of 26 μm between the sections were analyzed by LA-ICP-MS imaging to study elemental distribution in the wheat embryo. Those sections represent the wheat embryo from the root primordia to the leaf primordia (Fig. 1a). The registration of these successive wheat sections provided information on elemental distribution along the perpendicular axis of the wheat grain. The simplified three-dimensional images of each nutrient allowed us to conceive the changes of each element at different spatial levels (see ESI†). Taking Mo as an example, at the level of the root primordia, Mo was enriched in the root primordium, while at the level of lateral roots, Mo was enriched in the cortex of these lateral roots. In contrast, other elements such as Mn, Fe and P did not show significant spatial distribution. Average Zn concentration in leaf primordia was about 100 μg g^{-1} ($n = 6$) higher than that in root primordia, while Cu concentration did not vary considerably (at 9.0 ± 0.6 and 8.4 ± 0.5 μg g^{-1} ($n = 6$) in leaf and root primordia, respectively) (ESI,† Table S1). In contrast, Fe and Mn were enriched in the root primordia than in leaf primordia, especially Mn (180 ± 10 μg g^{-1} in root primordia and 20 ± 2 μg g^{-1} ($n = 6$) in leaf primordia) (ESI,† Table S1).

For a real comprehensive 3D modeling of the elemental distribution in the wheat embryo, the direct measurement on perpendicular sections is necessary. Additionally, computational registration and alignment with histology of the wheat embryo needs further development for better understanding elemental distribution and their bio-functions.

4. Discussion

Uptake and storage of nutrients is important during grain maturation. The enrichment of these nutrients in the wheat embryo is required for proper metabolism and development of the next generation during germination and growth. Because the filial organs of the developing grain are apoplasmically isolated from the maternal tissue, trans-membrane transport is necessary for micro-nutrient uptake. The transfer route into wheat grains of the elemental nutrients is thought to be similar to that of sucrose. Import into the developing grain is restricted to a single vascular bundle located at the crease bottom, extending across the whole length of the grain. The crease vein is thought to be the site of phloem unloading.[33] Alternative transport pathways are prevented by cuticle formation within the cell walls of integuments surrounding the developing endosperm, except at the crease vein area.[34] Nucellar projection cells proximal to the endosperm represent the cellular sites of efflux whereas endosperm transfer cells (ETCs) form the uptake site into the filial grain part. Both nucellar projection and ETCs develop transfer cell morphology with wall ingrowths to amplify the transport-effective membrane surface.[35,36]

Our LA-ICP-MS imaging results show that some elements such as Mn, Mo and Cu accumulate in the crease region, probably within the vascular bundle and/or the nucellar projection. This indicates limited transfer rates between the crease and the endosperm, which may result from the low sink capacity in the endosperm.[37] Limited transfer could be due to the absence of specific transporters in the endosperm. In barley grains, the vacuolar transporter VIT1 is expressed in the embryo but not in the endosperm indicating a lack of Zn transport deeper into the endosperm.[38] In contrast to the endosperm, gene expression of element transporters is much higher in the aleurone and the embryo, which may explain the strong accumulation of most elements in these organs.

The presence of metal-chelating complexes can also affect the organ-specific accumulation. Improving sink strength in the rice endosperm by overexpression of ferritin[39] and nicotianamine synthase[40] leads to higher Fe concentrations. Our study clearly identifies the scutellum as a very efficient uptake, accumulation, and storage organ for nutrients such as Cu, Fe, K, Mg, Mn, P and Zn. It has been speculated that the scutellar epidermis develops transfer cells analogous to the endospermal transfer cells.[41] However, details are unknown and future analysis should unravel the underlying mechanisms of micro-element transport, uptake and storage into the scutellum.

Protein bodies within the different grain tissues show considerable structural diversity. Mineral reserves are mainly located within electron-dense globoid crystal portions of protein bodies. However, distinct globoid crystals are predominantly found in the protein bodies of the aleurone and embryo cells but are lacking in starchy endosperm protein bodies.[42] This could explain the preferential accumulation of the elements within the aleurone and the embryo but not in the starchy endosperm. The finding was confirmed by studying element accumulation in mature wheat grains, which was found to be very specific and to correlate well with distribution of globoid crystals.[43]

In the present study the distribution of P reveals a very distinct pattern in wheat grains, exclusively limited to the aleurone and the embryo. In rice, most of the P translocated from source organs is shown to be immediately converted into phytic acid (inositol hexakisphosphate, InsP6), which is a strong chelator of metal cations. Upon binding, phytate is formed, a salt of InsP6.[44] Phytate accumulates within protein bodies and is mainly concentrated in globoids, which are present in the aleurone cells.[45] To form phytate, P and chelating elements must be co-located. Our study clearly shows that predominantly K, Cu, Mg and Fe revealed a remarkable common distribution pattern with P. Such co-localization of P with elements such as K, Cu, Mg, and Fe may therefore reflect the distribution pattern of phytic acid and can also explain the strong tissue-specific distribution within the aleurone and the embryo. As an example of such co-localization, most Fe was found inside the chloroplasts instead of storage vacuoles under phosphate deficiency, most probably associated with ferritins.[46]

Zinc, on the other hand, shows a somewhat different distribution pattern and is also partially located in the starchy endosperm, particularly in regions near the embryo. It has been shown that in rice Zn binds loosely to InsP6 and accumulates not only in phytate but is bound mainly to S within proteins.[45] Accordingly, the distribution of S is different from that of most other elements. It is the only element enriched in the starchy endosperm with a downhill gradient towards the inner regions. The presence of S within the endosperm may reflect the co-localization with S-rich storage proteins.

Different elemental distributions obviously mirror its specific usage during germination and growth. For example, K is important for early growth processes, turgor maintenance and cell elongation. Similarly, Zn is required for nucleic acid transcription, processing and translation occurring during early growth processes. Accordingly, K and Zn are co-localized in the primordia of leaves and roots indicating an important role in these meristematic tissues. In contrast, levels of Mn, Mg and Fe are relatively low in primordial organs indicating their vacuolar localization and chelation with phytate. Preferential usage in growth is also evident from the different mobilization rates during germination.[47] Whereas mobilization of Zn and K is high, that of Fe and Mn is relatively low. This is in accordance with the preferential distribution of K and Zn within the leaf and root primordia in the present work and suggests a critical role in either meristematic or vascular tissues.[47] In contrast, Fe and Mn may be localized preferentially in storage tissues within vacuoles rather than in primordial organs.

5. Conclusion

The LA-ICP-MS imaging technique was used for visualizing the distribution of macro- and micro-elements within the embryo region of the developing wheat grain. Quantitative elemental images clearly showed that the wheat embryo contained a much higher concentration of most of the nutrients. In the embryo, the scutellum was found to be the primary sink for all the elements measured. Two sections at the level of root primordia and of leaf primordia were shown to illustrate the elemental distribution pattern, which indicated diverse metal accumulation. A successive visualization of the distribution pattern for each element was reconstructed by compilation of 34 cross sections, which provided the information on the spatial distribution of the elements along the perpendicular axis. Further studies are required to explore the mechanisms underlying transport and accumulation of nutrients in particular cell types.

Abbreviations

AL	Aleurone
COL	Coleoptile
COZ	Coleorhizae
DAF	Days after flowering
ETCs	Endospermal transfer cells
LA-ICP-MS	Laser ablation inductively coupled plasma mass spectrometry
LP	Leaf primordia
MVB	Main vascular bundle
NP	Nucellar projection
RP	Root primordia
SC	Scutellum
SCO	Seed coat
SE	Starchy endosperm

Acknowledgements

The authors would like to acknowledge Deutsche Forschungsgemeinschaft (DFG grant number BE 2649/5-1) for instrumental support of the BrainMet laboratory at Forschungszentrum Jülich (FZJ). Thermo Fisher Scientific, Bremen, Germany, is acknowledged for instrumental support. We thank Uta Siebert, IPK Gatersleben, for excellent technical assistance in preparing the tissue section, and Dr Andreas Matusch, Institut für Neurowissenschaften und Medizin (INM), FZJ, for the support of the 3D modeling.

References

1 R. Hänsch and R. R. Mendel, *Curr. Opin. Plant Biol.*, 2009, **12**, 259–266.
2 C. Curie, G. Cassin, D. Couch, F. Divol, K. Higuchi, M. Le Jean, J. Misson, A. Schikora, P. Czernic and S. Mari, *Ann. Bot.*, 2009, **103**, 1–11.
3 T. J. Stomph, E. Y. Choi and J. C. R. Stangoulis, *Ann. Bot.*, 2011, **107**, 927–937.
4 E. Lombi, E. Smith, T. H. Hansen, D. Paterson, M. D. de Jonge, D. L. Howard, D. P. Persson, S. Husted, C. Ryan and J. K. Schjoerring, *J. Exp. Bot.*, 2011, **62**, 273–282.
5 J. S. Becker, *Inorganic Mass Spectrometry: Principles and Application*, Wiley, Chichester, 2007.
6 J. S. Becker, M. Zoriy, A. Matusch, B. Wu, D. Salber, J. C. Palm and J. S. Becker, *Mass Spectrom. Rev.*, 2010, **29**, 156–175.
7 R. W. Hutchinson, A. G. Cox, C. W. McLeod, P. S. Marshall, A. Harper, E. L. Dawson and D. R. Howlett, *Anal. Biochem.*, 2005, **346**, 225.
8 M. Zoriy, A. Matusch, T. Spruss and J. S. Becker, *Int. J. Mass Spectrom.*, 2007, **260**, 102–106.
9 E. Moreno-Gordaliza, C. Giesen, A. Lázaro, D. Esteban-Fernández, B. Humanes, B. Cañas, U. Panne, A. Tejedor, N. Jakubowski and M. M. Gómez-Gómez, *Anal. Chem.*, 2011, **83**, 7933–7940.
10 A. Matusch, L. S. Fenn, C. Depboylu, M. Klietz, S. Strohmer, J. A. McLean and J. S. Becker, *Anal. Chem.*, 2012, **84**, 3170–3178.
11 B. Wu, M. Zoriy, Y. X. Chen and J. S. Becker, *Talanta*, 2009, **78**, 132–137.
12 M. A. O. da Silva and M. A. Z. Arruda, *Metallomics*, 2013, **5**, 62–67.
13 N. Weichert, I. Saalbach, H. Weichert, W. Weschke and H. Weber, *Plant Physiol.*, 2010, **152**, 698–710.
14 T. I. Baskin, C. H. Busby, L. C. Fowke, M. Sammut and F. Gubler, *Planta*, 1992, **187**, 405–413.

15 T. Osterholt, D. Salber, A. Matusch, J. S. Becker and C. Palm, *Int. J. Mass Spectrom.*, 2011, **307**, 232–239.
16 W. Weschke, R. Panitz, N. Sauer, Q. Wang, B. Neubohn, H. Weber and U. Wobus, *Plant J.*, 2000, **21**, 455–467.
17 G. H. Lyons, Y. Genc, J. C. R. Stangoulis, L. T. Palmer and R. D. Graham, *Biol. Trace Elem. Res.*, 2005, **103**, 155–168.
18 www.Mühlenchemie.de.
19 J. W. Patrick and C. E. Offler, *J. Exp. Bot.*, 2001, **52**, 551–564.
20 P. J. White and M. R. Broadley, *Ann. Bot.*, 2003, **92**, 487–511.
21 O. Shaul, *BioMetals*, 2003, **15**, 309–323.
22 S. Luan, W. Lan and S. C. Lee, *Curr. Opin. Plant Biol.*, 2009, **12**, 339–346.
23 C. A. Hebbern, K. H. Laursen, S. B. Ladegaard, S. B. Schmidt, P. Pedas, D. Bruhn, J. K. Schjoerring, D. Wulfsohn and S. Husted, *Physiol. Plant.*, 2009, **135**, 307–316.
24 I. Yruela, *Metallomics*, 2013, DOI: 10.1039/C3MT00086A.
25 U. Kramer and S. Clemens, *Top. Curr. Genet.*, 2005, **14**, 215–271.
26 M. Tejada-Jimenez, A. Chamizo-Ampudia, A. Galvan, E. Fernandez and A. Llamas, *Metallomics*, 2013, DOI: 10.1039/C3MT00078H.
27 G. Schwarz and R. R. Mendel, *Annu. Rev. Plant Biol.*, 2006, **57**, 623–647.
28 T. Mimura, *Plant Cell Physiol.*, 1994, **36**, 1–7.
29 G. E. Ravilious and J. M. Jez, *Nat. Prod. Rep.*, 2012, **29**, 1138–1152.
30 H. Marschner, *Mineral Nutrition of Higher Plants*, Academic Press Inc., San Diego, CA 92101, 1995, pp. 313–340.
31 D. G. Blevins and K. M. Lukaszewski, *Annu. Rev. Plant Physiol. Plant Mol. Biol.*, 1998, **49**, 481–500.
32 P. J. White and M. R. Broadley, *Ann. Bot.*, 2001, **88**, 967–988.
33 J. H. Thorne, *Ann. Rev. Plant Physiol.*, 1985, **36**, 317–343.
34 S. Y. Zee and T. P. O'Brien, *Aust. J. Biol. Sci.*, 1970, **23**, 1153–1171.
35 H. L. Wang, C. E. Offler and J. W. Patrick, *Protoplasma*, 1994, **182**, 39–52.
36 W. Weschke, R. Panitz, N. Sauer, Q. Wang, B. Neubohn, H. Weber and U. Wobus, *Plant J.*, 2000, **21**, 455–467.
37 T. J. Stomph, E. Y. Choi and J. C. Stangoulis, *Ann. Bot.*, 2011, **107**, 927–937.
38 B. Tauris, S. Borg, P. L. Gregersen and P. B. Holm, *J. Exp. Bot.*, 2009, **60**, 1333–1347.
39 F. Goto, T. Yoshihara, N. Shigemoto, S. Toki and F. Takaiwa, *Nat. Biotechnol.*, 1999, **17**, 282–286.
40 W. H. Zhang, Y. Zhou, K. E. Dibley, S. D. Tyerman, R. T. Furbank and J. W. Patrick, *Funct. Plant Biol.*, 2007, **34**, 314–331.
41 M. Salmenkallio and T. Sopanen, *Plant Physiol.*, 1989, **89**, 1285–1291.
42 J. N. Lott and E. Spitzer, *Plant Physiol.*, 1980, **66**, 494–499.
43 A. P. Mazzolini, C. K. Pallghy and G. J. F. Legge, *New Phytol.*, 1985, **100**, 483–509.
44 V. Raboy, *Plant Sci.*, 2009, **177**, 281–296.
45 T. Iwai, M. Takahashi, K. Oda, Y. Terada and K. T. Yoshida, *Plant Physiol.*, 2012, **160**, 2007–2014.
46 A. Pich, R. Manteuffel, S. Hillmer, G. Scholz and W. Schmidt, *Planta*, 2001, **213**, 967–976.
47 L. Lu, S. Tian, H. Liao, J. Zhang, X. Yang, J. M. Labavitch and W. Chen, *PLoS One*, 2013, **8**, e57360.

